

# Coated glass beads epoxy composites: influence of the interlayer thickness on pre-yielding and fracture properties

N. AMDOUNI, H. SAUTEREAU, J. F. GERARD

*Laboratoire des Matériaux Macromoléculaires – UA CNRS 507, INSA, Bâtiment 403, 69621 Villeurbanne, France*

F. FERNAGUT, G. COULON, J. M. LEFEBVRE

*Laboratoire des Structures et Propriétés de l'Etat Solide – UA CNRS 234, Université des Sciences et Techniques de Lille Flandres Artois, 59655 Villeneuve D'Ascq, France*

An elastomeric adduct based on a liquid rubber, an epoxy prepolymer and a liquid diamine has been prepared and deposited around glass beads reinforcing an epoxy matrix. The pre-yielding and fracture properties of such composites are studied and compared with those of untreated glass beads based composites. A linear dependence of  $K_{Ic}$  (critical stress intensity factor) versus volume fraction is obtained for untreated glass beads composites, whereas a maximum is reached at 20% volume fraction of filler for those with coated glass beads. Introduction of an elastomeric layer improves fracture toughness and the influence of interlayer thickness is studied. A maximum for  $K_{Ic}$  is found for  $(e/r) = 3\%$  in connection with a strong decrease of  $K/M$  ratio (work-hardening rate compression modulus) determined in the pre-yielding stage. The toughening mechanism is discussed primarily in terms of crack pinning and plastic deformation.

## 1. Introduction

Much work has been done on particulate-filled epoxy networks and their mechanical behaviour depends on the properties of the different constituents: matrix, filler and interface (or interphase). It is now well established that the principal parameters determining strength and toughness are: volume fraction of filler [1–6], particle size [1–2, 5–7] and surface treatments [2–6, 8–9]. The influence of these parameters has recently been reviewed by Young [10].

The failure of these composite materials, both in static fatigue and impact tests, almost always occurs from micro-defects or inhomogeneities in the bulk material or at the filler/matrix interface which induce stress concentration.

Different ways have been investigated of enhancing the fracture toughness of reinforced thermosets. The most widely used methods are the improvement of the epoxy network itself and/or the increase of the filler/matrix adhesion.

In the first case, the use of a second rubbery phase was described by Sultan and McGarry [11], and since then numerous works have been done on rubber modified thermosets. This concept is used in hybrid-particulate composites [5, 12, 13]. For example, Maxwell [14] demonstrated that the toughening mechanisms are optimized and that the materials have an improved resistance to crack propagation. Kausch and colleagues [6] note an increase of stress intensity factor and fracture energy by factors of about 2.5 and

4.5 respectively on hybrid resin systems compared to those without a rubber phase. However, the strength and the modulus are strongly reduced (about 30% on flexural strength).

In the second case, coupling agents were used to increase filler/matrix adhesion. No significant improvement is displayed [2–6]; on the contrary, higher toughness is observed with poorly bonded filler (mould release agent for example) [4]. This phenomenon [1, 2] could be explained by crack tip blunting with poorly bonded particles acting as sources of "inherent" flaws.

An intermediate way is the encapsulation of fillers with a controlled modulus interlayer which is able to give a tougher composite without losses in strength and stiffness [15]. The insertion of a soft interphase at the particulate surface could be justified by theoretical studies and problem of residual stresses after curing of the thermoset matrix.

(a) Theoretical analysis developed on particulate and fibre composites [15, 16] has shown that the toughness of the material can be maximized by controlling the thickness and modulus of the interlayer. Micromechanical analysis of such materials with coated filler and a glassy matrix predicted a modification of the stress distribution around the particles as a function of elastic constants and volume fraction of the interface layer [16–17]. A few experiments conducted on glass bead composites confirm the theoretical predictions of sites of craze formation [18–20].

(b) DiBenedetto and Nicolais [21] attributed the

effectiveness of a flexible interlayer to stress relief in the interphase region. Residual stresses are accumulated during curing and shrinkage of the matrix according to the large difference in thermal expansion coefficients of the dispersed phase and matrix. Usually in filled epoxies the glass beads undergo compression [22], and the deposition of a thin elastomeric interlayer around the filler both induces a decrease in compression stresses and modifies the stress distribution [16].

Many experiments address the problem of embedding the filler in a thin rubbery interlayer either in the case of glass beads [18–20] or glass or carbon fibres [23–25].

In the present work, we choose the approach of Riess *et al.* [25] who use block copolymers for the preparation of the elastomeric interphase. This one is based on flexible segments (CTBN – carboxy terminated butadiene acrylonitrile copolymer) and segments compatible with an epoxy matrix. The chemical and coating processes have been described previously [26]. The influence of such an interphase on the properties of composites materials based on glass beads [27] and carbon fibres [28] has been reported previously.

In this paper, we study the influence of interlayer thickness on mechanical properties of coated glass beads epoxy composites. The deformation mechanisms of epoxy matrix are considered using a metallurgical approach and through measurements obtained using linear elastic fracture mechanics ( $K_{Ic}$  and  $G_{Ic}$ ) are obtained as a function of the interlayer thickness, the volume fraction of glass beads and the particle size. These results are compared with theoretical studies.

## 2. Experimental procedures

### 2.1. Materials

#### 2.1.1. Preparation of the elastomeric adduct

The elastomeric interlayer is prepared in a two stages process from a carboxy terminated butadiene acrylonitrile copolymer (CTBN), an epoxy prepolymer (DGEBA – diglycidyl ether of bisphenol A) and a liquid hardener (IPD). These products are described in Table I. In the first stage, the reaction between DGEBA and CTBN is carried out at 85°C (stoichiometric ratio = 0.5) under vacuum and mechanical

stirring with 0.15% (by weight) of triphenyl phosphine as catalyst. This reaction has been described in a previous paper [26]. After a reacting time of 20 h IPD, a liquid diamine, chosen for the large difference between its primary and secondary amine reactivities is added at 20°C (stoichiometric ratio = 2). At this temperature, only primary amine functions react with epoxy groups and chain extension occurs. After 19 h of reaction, the product is soluble in methyl ethyl ketone (MEK) and could be deposited onto glass beads by the solvent coating process. After removal of MEK by heating, secondary amine and epoxy groups which are still present could react and achieve the crosslinking of the adduct around the filler. The chemical characterization of this CTBN–DGEBA–IPD adduct is described in a paper to be published [29].

#### 2.1.2. Surface treatment of glass beads

Glass beads, with particle sizes ranging from 4 to 44  $\mu\text{m}$  from SOVITEC (A050) are used. In order to study the particle size influence, larger beads (in the range 105 to 200  $\mu\text{m}$ ) are also introduced. Two kinds of surface beads treatment are studied: no treatment and adduct coated.

Glass beads are mixed with the adduct dissolved in MEK at room temperature. Different amounts of elastomer are used to obtain the different thicknesses of interlayer. MEK is removed after mixing for 20 min and the glass beads are then dried under vacuum at 120°C for 12 h. At this temperature, MEK is completely removed and the adduct crosslinks around the glass beads.

The chemical characterization of the (DGEBA–CTBN–IPD) deposit is made directly on the glass beads before adding them to the matrix. A FT-IR Nicolet MX-1 spectrometer equipped with a diffused reflection device (DRIFT) is used for this study. After the crosslinking process epoxy groups are still present (910  $\text{cm}^{-1}$  band on IR spectrum). These functions are able to react with amine groups of the matrix during the curing of the composite. The weight fractions of coating ( $\tau_a$ ) determined using thermogravimetric analysis at 625°C (listed in Table II) allow us to

TABLE I Synthesis of the elastomeric adduct

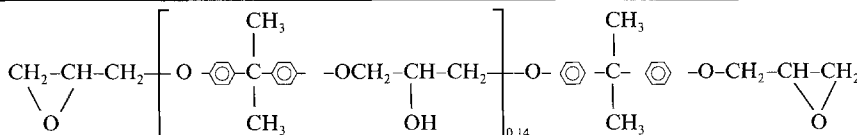
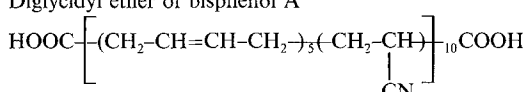
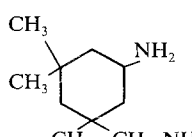
Product	Supplier	Formula	
DGEBA	Bakelite 0164		$\bar{M}_n = 380 \text{ g}$
CTBN	Hycar 1300 $\times$ 8 Goodrich		$\bar{M}_n = 3500 \text{ g}$
IPD	Hüls		Isophorone diamine

TABLE II Weight fractions  $\tau_A$  of elastomer on glass beads and calculation of average  $(\overline{e/r})$  ratios according to the distribution of glass beads diameters

Concentration of the MEK solution (wt %)	$\tau_A$ (wt %)	$(\overline{e/r})$ (%)	SD ( $e/r$ ) (%)
1.1	0.9	2.0	0.3
1.8	1.7	2.8	0.6
3.4	3.2	4.2	1.0
5.8	5.6	6.5	1.8

compute the  $e/r$  ratios (thickness of the interlayer/radius of the glass bead).

In order to calculate the ratio  $e/r$  for each concentration of elastomer in MEK, it is necessary to take into account the distribution of glass beads diameters. The assumption underlying this calculation is that the elastomer settles uniformly in an amount proportional to the surface area of the glass particles. So for each fraction  $i$  of the population we compute  $(e/r)_i$ , and  $(\overline{e/r})$ , the average of the  $(e/r)_i$  distribution, as well as its standard deviation SD ( $e/r$ ) is obtained. The detailed calculation will be described elsewhere.

### 2.1.3. Preparation of composites

Composite materials are prepared from untreated or coated glass beads and an epoxy matrix. The latter is based on an epoxy prepolymer DGEBA (described in Table I) and dicyandiamide (dicy.) with BDMA (benzyl dimethyl amine) as an accelerator. The stoichiometric ratio amine-to-epoxy is fixed at 0.6 in order to achieve maximum of  $T_g$  (glass transition temperature) [30]. The mixture of glass beads and epoxy is cured in a rotated PTFE-coated mould for 1 h at 120°C and 1 h at 180°C. Differential scanning calorimetry (DSC) shows that under these conditions, the reaction is complete: no residual exothermal effect is detected and the glass transition temperature remains constant. The various volume fractions of filler studied here are checked by burning off the resin.

For the composites based on coated particles, the presence of the elastomeric layer around glass beads in the composite material is displayed in the dynamic mechanical spectra (damping  $\tan \delta$  and storage modulus  $E'$  against temperature and frequency). At low frequency (about 0.1 Hz), two peaks in the loss factor  $\tan \delta$  versus  $T$  spectrum are resolved and identified, one due to the secondary relaxation of the epoxy matrix network ( $-57^\circ\text{C}$ ) [29]. So the adduct truly exists as a third phase and the composite material could be described as a three phase material. This technique has been used previously for coated glass bead [26] and coated carbon fibre [28] composites.

## 2.2. Mechanical tests

### 2.2.1. Linear elastic fracture mechanics

Single-edge notched specimens (SEN) (thickness  $t \sim 6$  mm and width  $w \sim 12$  mm) are prepared and tested in three-points bending mode (span-to-length is 48 mm). Cracks of length  $a$  are machined with a saw and the crack tip is achieved with a razor blade at 170°C (above  $T_g$ ). About 12 notched specimens with various  $a/w$  are fractured (cross-head speed = 1 mm

min<sup>-1</sup>). Fracture toughness ( $K_{Ic}$ ) is calculated using the following formula:

$$K_{Ic} = \sigma_c (\pi a)^{1/2} f(a/w)$$

where  $\sigma_c$  is the critical stress for crack propagation (in this case, the stress at break) and  $f(a/w)$  the form factor [31].

The fracture energy  $G_{Ic}$  may be related [31] to the stress-intensity factor  $K_{Ic}$  in plane strain conditions by the equation

$$G_{Ic} = \frac{K_{Ic}^2}{E} (1 - \nu^2)$$

where  $\nu$  is the Poisson coefficient and  $E$  the Young's modulus of the material. For the composite material  $\nu$  is obtained from a volumic rule of mixture (with  $\nu_{\text{glass}} = 0.21$  and  $\nu_{\text{matrix}} = 0.33$ ).

Young's moduli  $E$  are obtained from a tensile test at room temperature on an Adamel-Lhomargy (DY 25) machine. Strain measurements are performed with an EX10 extensometer at a strain rate of  $3.3 \times 10^{-4} \text{ sec}^{-1}$ .

### 2.2.2. Measurements of the non-elastic work-hardening rate

The micromechanical characterization consists in measuring the non-elastic work-hardening rate  $K$  in the pre-yield stage during compression tests at constant strain rate  $\dot{\epsilon}$ . This method has been already described in previous papers [32–34].

The non-elastic work-hardening  $K$  can be defined as

$$K = \left[ \frac{\partial \sigma_a}{\partial \epsilon_p} \right]_{i,T}$$

where  $\sigma_a$  is the applied stress,  $\epsilon_p$  is the resulting non-elastic strain of the material and  $\dot{\epsilon}$  the total strain rate.

From a metallurgical point of view, we consider the nucleation of shear defects in the macromolecular arrangement.  $K$  is related to the nucleation rate of defects per unit stress as

$$K = \left[ \frac{dN}{d\sigma_a} \right]_{i,T}^{-1}$$

where  $dN$  is the number of defects created by the stress increment  $d\sigma_a$ ; the nucleation of these  $dN$  defects is responsible for the non-elastic strain  $d\epsilon_p$  in the solid.  $K$  is thus a measure of the resistance of the material to develop plastic strain: the higher the  $K$ , the less the material is able to deform plastically.

The evaluation of  $K$  requires two different tests conducted at the same  $\epsilon_p$ . A single stress relaxation test leads to  $V_{\text{exp}}$ , the experimental activation volume

$$V_{\text{exp}} = V_0 \left( 1 + \frac{K}{M} \right)$$

where  $V_0$  is the apparent activation volume and  $M$  is the sample-machine elastic modulus.

In a repeated stress relaxation test, the sample is repeatedly relaxed by the same stress drop  $\Delta\sigma_0$ : if  $\Delta t_1$  and  $\Delta t_n$  are the duration of the first and  $n$ th relaxations respectively, a plot of  $\ln(\Delta t_n/\Delta t_1)$  against  $(n-1)$  yields a straight line with slope  $V_0 K/M$ . Combining

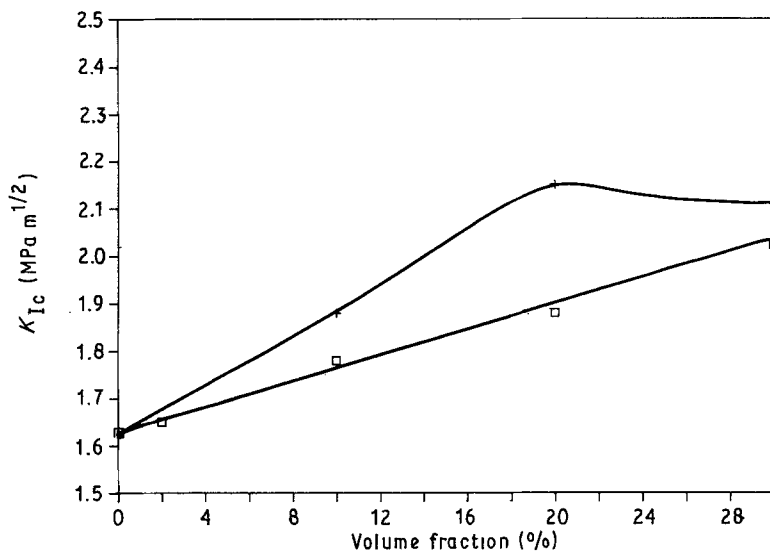


Figure 1 Critical stress-intensity factor  $K_{Ic}$  as a function of volume fraction of glass beads: ( $\square$ ) untreated and ( $+$ ) coated with 3.2 wt % of elastomer (see also Table IV).

both experiments finally gives  $K/M$ :

$$\frac{K}{M} = \frac{V_0 K/M}{V_{exp} - V_0 K/M}$$

Compression tests at a constant rate  $\dot{\epsilon} = 2 \times 10^{-4} \text{ sec}^{-1}$  are performed using an Instron 1195 machine on cylindrical specimens (9.2 mm long and with 5 mm diameter). The measurements are made at a non-elastic strain  $\epsilon_p = 5 \times 10^{-3} \cdot V_0 K/M$  is obtained from twelve successive relaxations with a stress decrement of about 15 N.

### 2.3. Fractography

The fracture surfaces of broken SEN specimens are examined using a JEOL 840 A scanning electron microscope (operated at 15 kV). They were sputter-coated before observation with a thin layer of gold.

## 3. Results and discussion

### 3.1. Effect of the volume fraction of glass beads on the fracture properties of composites

The effect of the volume fraction of filler on the mechanical properties of epoxy composites has been studied extensively [1, 5–7, 10, 35]. Many theoretical studies have been developed to determine the modulus of composite materials from the characteristics of each component. Young's moduli ( $E$ ) obtained from tensile tests are given in Table III and will be discussed

in detail elsewhere [29]. The increase of  $E$  with volume fraction of untreated or coated glass beads (with 3.2 wt % elastomer) is in agreement with those reported in the literature [5]. The introduction of an elastomeric interlayer slightly reduces the modulus of the composite (for example, with 20% volume fraction of glass,  $E$  is about 6% lower for glass beads coated with 3.2 wt % adduct). A typical increase of yield stress in compression is also observed with the volume fraction ( $v_g$ ) of glass beads [1, 13, 36, 37].

Similarly, increasing the volume fraction of untreated glass beads increases the stress intensity factor ( $K_{Ic}$ ) as shown in Fig. 1. A linear variation of  $K_{Ic}$  versus  $v_g$  is observed for the untreated glass beads based composites. This result is also in agreement with other data reported in the same range of filler fraction [1, 2, 5, 27, 37].

The fact that Young's modulus increases faster than  $K_{Ic}$  with  $v_g$  induces a maximum for fracture energy  $G_{Ic}$ . This value  $G_{Ic}(\text{max})$  occurs for about 10% of untreated glass beads (Fig. 2).

These results are usually interpreted [1, 10] in terms of crack front pinning, a mechanism previously described by Lange and Radford [38]. In our case, the yield stresses of the pure matrix (105 MPa) [39], and obviously of the filled networks, are higher than 100 MPa, which constitutes a critical value proposed by Kinloch and Williams [40] to explain the transition between unstable (stick-slip) and stable propagation.

TABLE III Young's moduli  $E$  (tensile test) and yield stresses  $\sigma_y$  (uniaxial compression) for the composite materials and matrix

Formulation of the composites	Volume fraction of glass (%)	Interlayer thickness ( $\bar{e}/r$ ) (%)	$E$ (GPa)	$\sigma_y$ (MPa) ( $\dot{\epsilon} = 2.10^{-4} \text{ sec}^{-1}$ )
(DGEBA-DDA) matrix precured 1 h at 120°C	0	–	2.92	105
C (2, 0)	2*	0	3.08	107
C (20, 0)	20*	0	4.78	119
C (20, 2)	20*	2	4.6	114
C (20, 2.8)	20*	2.8	4.54	115
C (20, 4.2)	20*	4.2	4.48	113
C (20, 6.5)	20*	6.5	4.35	115
C (20L, 0)	20†	0	4.8	114

\*Glass beads with sizes between 4 and 44  $\mu\text{m}$ .

†Glass beads with sizes between 105 and 210  $\mu\text{m}$ .

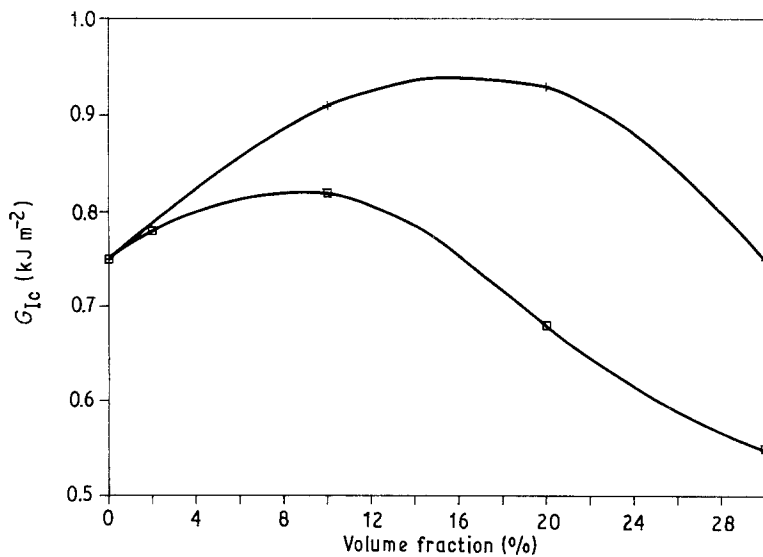


Figure 2 Fracture energy  $G_{Ic}$  as a function of volume fraction of glass beads: (□) untreated and (+) coated with 3.2 wt % of elastomer (see also Table IV).

As seen on the fracture surfaces, in contrast to the observations of Roulin-Moloney and colleagues [41], only few decohesions occur around untreated glass beads and some epoxy even remains attached to the particles. The untreated glass surface appears sufficiently reactive to promote adhesion with (DGEBA-DDA) matrix. The efficiency of crack pinning is improved by adhesion; on the other hand, crack blunting is favoured by non-adhesion. So the values of  $K_{Ic}$  and  $G_{Ic}$  are a result of a competition between these two mechanisms with an evident dominance of crack pinning in the conditions of our study.

The  $K$  factors (of filled and unreinforced matrix) cannot be directly compared because even the same overall plastic deformation  $\epsilon_p$ , the real  $\epsilon_p$  of the matrix is increasing with  $v_g$ . The same discussion could be applied to the yield stresses which are not related to the volume fraction of the deformed matrix. In addition, localized plastic deformation can take place simultaneously with crack pinning [10, 12]. Glass particles can act as nucleation sites for shear deformation in the epoxy matrix, so toughness can be increased through this mechanism.

In the case of coated glass beads ( $e/r = 4.2\%$ ),  $K_{Ic}$  displays a maximum at about 20% volume fraction of filler. This result is similar to the observations in

hybrid particulate composites [5, 6, 10, 12].  $G_{Ic}$  also goes through a maximum for 15% volume fraction of glass beads. In hybrid particulate composites, toughening mechanisms generally considered are (1) crack pinning with same way as in epoxy-filler composites and (2) localized plastic deformation around cracks induced by the rubber particles [12]. This mechanism leads to a rougher fracture surface. For these composites, deformation processes reported are cavitation in the rubber or/and at the particle matrix interface and multiple but localized plastic shear yielding in the matrix in the vicinity of the rubber nodules [12, 41, 42]. Extra shear deformation can also be initiated by glass particles [12].

In the case of coated glass beads/epoxy matrix composites, the localization of the rubber is different but these mechanisms could explain the observed fracture properties. The fracture surface of these composites (see Fig. 5, below) shows "tails" characteristic of a crack pinning mechanism behind the filler, as in uncoated glass bead based composites. But the main phenomena are multiple secondary cracks in the matrix and local plastic deformation near coated particles. This assumption is confirmed by the decrease of yield stress (Table III) due to the presence of the coating for 20% volume fraction of glass beads. These

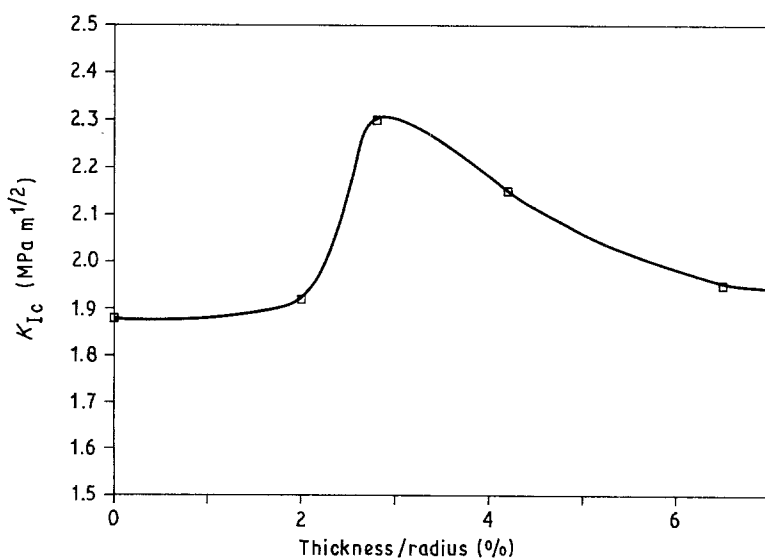


Figure 3 Critical stress-intensity factor  $K_{Ic}$  as a function of interlayer thickness on the glass beads (composite materials based on 20% volume fraction of filler).

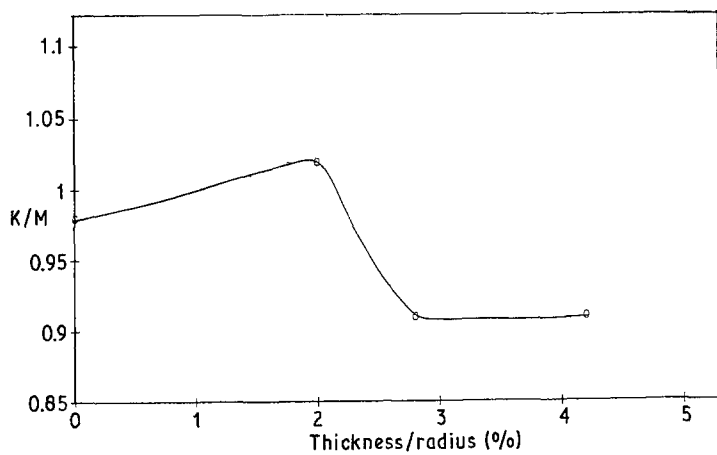


Figure 4  $K/M$  ratio against the interlayer thickness on the glass beads (composite materials based on 20% volume fraction of filler).

phenomena are discussed and explained in the next section of this paper, which deals with the influence of the thickness of the elastomeric interlayer.

The improvement of fracture of particulate composites induced by coating an elastomer around glass beads is very important (from 1.85 to 2.15 MPa m<sup>1/2</sup> for a 20% volume fraction composite and  $e/r = 4.2\%$ ) with only a slight decrease in elastic properties ( $E$  from 4.78 to 4.48 GPa). Such a surface modification of glass beads doesn't lead to a loss of thermal properties. The presence of the elastomeric interlayer decreases the glass transition temperature ( $T_g$ ) of 20% glass composites to 144 to 140° C (depending on the interphase thickness). A greater decrease of  $T_g$  value is generally recorded for hybrid particulate composites with 15% CTBN in the matrix.

According to the maxima observed for stress intensity factor ( $K_{Ic}$ , Fig. 1) and fracture energy ( $G_{Ic}$ , Fig. 2) against fraction ( $v_g$ ) of coated glass beads,  $v_g$  is fixed at 20% to study the dependence of fractures and pre-yielding properties on particle size and interlayer thickness.

### 3.2. Effect of the particle size on fracture and pre-yielding properties of composites

Measurements of mechanical properties ( $E$ ,  $\sigma_Y$ ), work hardening rate ( $K$ ) and crack-propagation behaviour ( $K_{Ic}$ ,  $G_{Ic}$ ) are made on composite materials with 20% (by volume) of untreated glass beads with two different size distributions (4 to 44  $\mu\text{m}$  and 105 to 215  $\mu\text{m}$  respectively) named C(20,0) and C(20L, 0). All data are reported in Tables III and IV.

Filler particle size at 20% volume fraction does not show any influence on the Young's modulus of the composite in agreement with the literature [1, 5]. A

slight decrease is observed for the stress intensity factor ( $K_{Ic}$ ) with increasing particle size. Generally, many workers [1, 5, 10] agree that the glass bead diameter ( $d$ ) has a secondary effect on the value of  $K_{Ic}$ . In our case, the 20% volume fraction of filler is between 10%, for which  $K_{Ic}$  decreases with  $d$ , and 30%, for which  $K_{Ic}$  is constant with  $d$  [1, 6]. The decrease of fracture energy with  $d$  is the same that for  $K_{Ic}$ . Varying particle size only influences stability of propagation [10].

Study of pre-yielding shows a decrease for the ratio  $K/M$  (work-hardening rate  $K$ /compressive modulus  $M$ ). From the point of view of deformation physics,  $K/M$ , measured in the pre-yielding stage, varies as the inverse of the defect nucleation rate and is greatly influenced by any change in meso-structure of the material.  $K/M$  values reported in Table V show that larger particle size leads to a stronger hardening of the material than the smaller glass beads. The work-hardening rate is thus a parameter which is very sensitive to any structural evolution at the scale of heterogeneities involved in the nucleation of plastic deformation. It is well-known that the underlying mechanism of plastic deformation in particulate-filled epoxies is shear yielding in the polymer matrix [13]. For this reason pre-yielding characteristics are affected by any change in deformation mechanisms around glass beads: particle size, bonding at the particle/matrix interface, etc. In addition, it was demonstrated that flaw sizes for such materials are of the order of 100  $\mu\text{m}$  [5], about the same size as the largest particles (105 to 215  $\mu\text{m}$ ).  $K$  is affected in the same way as strength by the higher probability of a flaw being present within the particle.

### 3.3. Effect of the interlayer thickness

In our study, the average ratio of elastomeric interlayer thickness to particle diameter ( $\bar{e}/r$ ) varies from 0 to 6.5%. The Young's modulus  $E$  is slightly reduced by the introduction of an elastomeric interlayer with a modulus lower than the matrix (4% reduction for C(20, 2)). For the same cure conditions as the filled composites, pure elastomeric adduct displays a Young's modulus equal to 0.5 MPa. Decrease of  $E$  is more important with increasing interlayer thickness (9% reduction for the maximum of  $e/r$  in C(20, 6.5)). This decrease is in agreement with theoretical studies of Matonis and Small [15]. Indeed, they observed that

TABLE IV Effect of the volume fraction of coated ( $\bar{e}/r = 4.2\%$ ) glass beads (size from 4  $\mu\text{m}$  to 44  $\mu\text{m}$ ) on the fracture properties ( $K_{Ic}$  and  $G_{Ic}$ ) of the composite materials

Nomenclature	Volume fraction of glass beads (%)	$K_{Ic}$ (MPa m <sup>1/2</sup> )	$G_{Ic}$ (kJ m <sup>-2</sup> )
(DGEBA-DDA)* (unfilled matrix)	0	1.63	0.8
C (10, 4.2)	10	1.88	0.91
C (20, 4.2)	20	2.15	0.93
C (30, 4.2)	30	2.11	0.75

\*Curing: 1 h at 120° C followed by 1 h at 180° C.

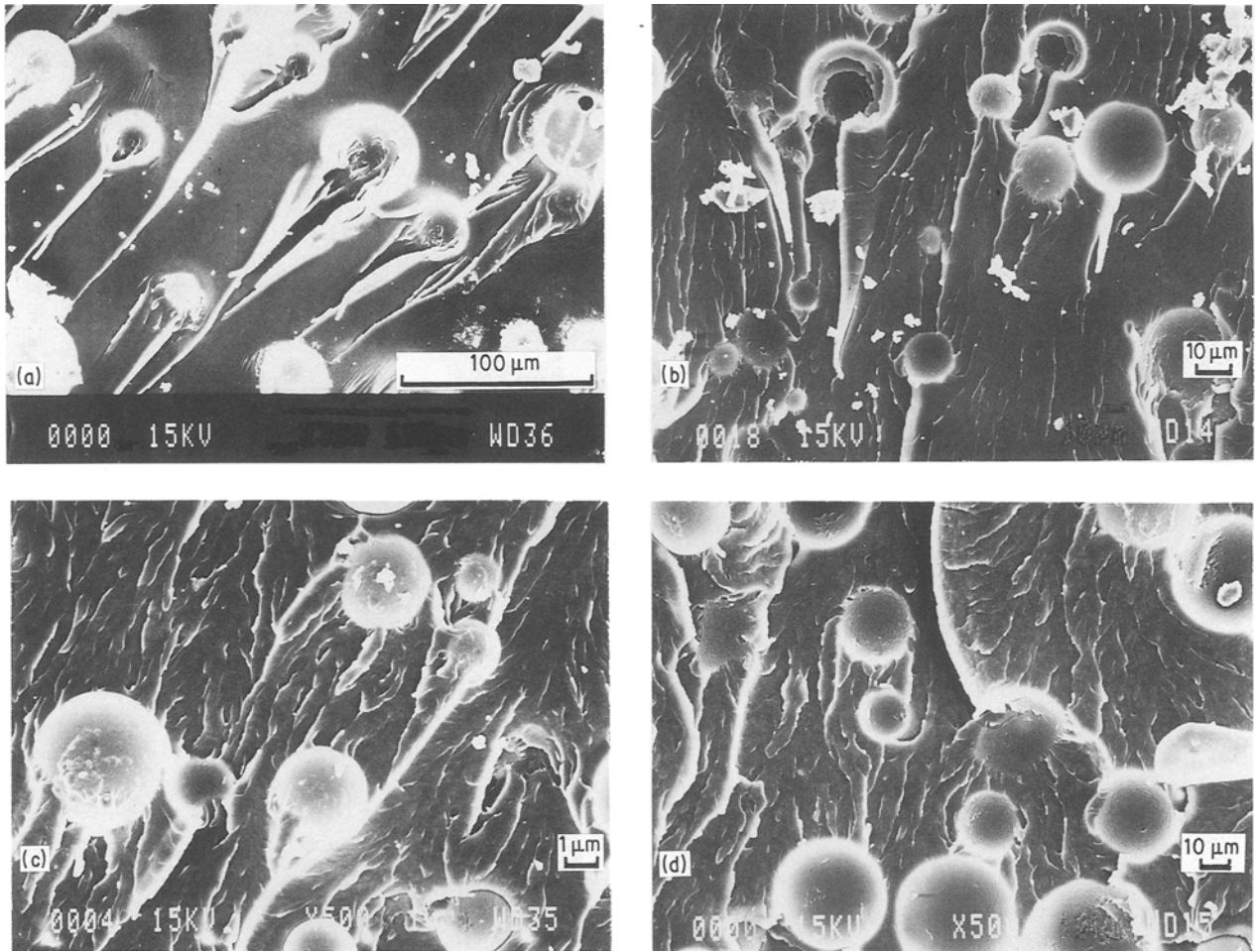


Figure 5 Micrographs of fracture surface of SEN specimens for different thicknesses of elastomeric interlayer (composites with 20% volume fraction of glass). (a) Untreated, (b)  $(e/r) = 2.0\%$ , (c)  $(e/r) = 2.8\%$ , (d)  $(e/r) = 6.5\%$ .

only very thin layers of rubber are admissible ( $e/r = 0.1\%$ ) and the use of slightly thicker layers ( $e/r = 4\%$ ) lowers the modulus. From a technological point of view, the decrease of modulus is allowable if the fracture behaviour is improved. Different theoretical models for predicting the Young's modulus of these composite materials will be considered in a forthcoming paper [29].

Yield stress  $\sigma_Y$  is in the range of 114 to 119 MPa for all the composites, whatever the thickness. So for these amounts and localization of rubber, yield stress doesn't suffer significantly in opposition to what is observed in hybrid-particulate composite (with for example 15% by volume of rubber CTBN [13]). As is demonstrated later, pre-yielding measurements offer a

more sensitive approach to the modification of deformation mechanisms induced by coating.

Crack propagation studies for the various epoxy composites with coated glass beads show the influence of interlayer thickness (Figs 3 and 4; Table V). Values of critical stress intensity factor and fracture energy ( $K_{Ic}$  and  $G_{Ic}$  respectively) display maxima at about 3% for  $e/r$ . The improvement of  $K_{Ic}$  is about 22% in comparison with uncoated filler based composite. Variation of  $G_{Ic}$  is more pronounced depending on the decrease in Young's modulus. The micromechanical analysis made by Ricco and colleagues [17] describes craze initiation factors for an elementary single model of a two phase particle embedded in an infinite matrix under uniform uniaxial tension. Although crazing is

TABLE V Effect of the interlayer thickness and size of the glass beads on the fracture properties ( $K_{Ic}$ ,  $G_{Ic}$ ) and pre-yield behaviour of the composite materials (20% volume of fraction filler)

Nomenclature*	Fracture		Pre-yielding	
	$K_{Ic}$ (MPa m <sup>1/2</sup> )	$G_{Ic}$ (kJ m <sup>-2</sup> )	$K/M$	$V_0$ (Å <sup>3</sup> )
C (2, 0) <sup>†</sup>	1.65	0.78	0.66	1350
C (20, 0) <sup>†</sup>	1.88	0.67	0.98	807
C (20, 2) <sup>†</sup>	1.92	0.72	1.02	802
C (20, 2.8) <sup>†</sup>	2.3	1.1	0.91	958
C (20, 4.2) <sup>†</sup>	2.15	0.93	0.91	879
C (20, 6.5) <sup>†</sup>	1.95	0.79	0.74	1184
C (20L, 0) <sup>‡</sup>	1.8	0.61	0.87	871

\* See Table III.

<sup>†</sup> Glass beads size distribution 4 to 44  $\mu\text{m}$ .

<sup>‡</sup> Glass beads size distribution 105 to 210  $\mu\text{m}$ .

not a deformation mechanism for epoxy networks, this analysis may be directly transposed in our case. In the region surrounding the heterogeneous particle, maximum principal stress, maximum principal strain, strain, dilation, strain energy density, maximum principal shear stress and distortion energy density are analysed as a function of the thickness of the rubber interlayer. These factors do not generally vary monotonically with the distance from the bead. For a thickness to radius ratio of about 4.2, the maximum principal stress is maximum at the pole of the particle. So the craze formation for this thickness is located either at the pole or at the equator of the particle. These theoretical conclusions were verified experimentally by Abate and Heikens [19]. In our case, the assumptions in Ricco's model are not fulfilled: the matrix is not infinite and is not subjected to a uniform uniaxial tensile stress, the size distribution of beads is not monodisperse and the calculations are made with the hypothesis that the ratio of elastomer to matrix modulus is about 1000. (In our case, it is about 6000.) In addition, the component occluded in the particle is not matrix but glass, in contrast to Ricco's model, and adhesion at the filler surface is not probably perfect. Another limit to apply to this model is that the two components are assumed to obey linear elasticity, and micromechanical analysis to predict craze initiation is only valid before the point of craze formation. As soon as crazing occurs, the material behaviour departs from this description.

In the pre-yield stage, the work-hardening rate is nearly constant up to  $e/r = 2\%$  and decreases rapidly (10% in relative value) between 2 and 2.8% (Fig. 4). Beyond these values,  $K/M$  seems to be constant. The decrease of  $K/M$  value means that the material is able to undergo more plastic deformation, since  $K$  is a measure of the resistance of the composite to plastic strain.

So in the pre-yield stage, beyond  $e/r = 2.8\%$ , the nucleation rate of defects is minimum. This observation is in agreement with the existence of an optimum interphase thickness, as demonstrated by Ricco and other authors: for instance Matonis and Small [15] calculated an optimum thickness for toughening at 4% and Pfeiffer and Nielsen [23], in the case of short glass fibres, reported an impact toughening for an optimum thickness about 6%. Thicknesses are not exactly the same for the reasons given above.

Micrographs of the fracture surfaces of SEN specimens clearly show rough surfaces with bumps and ridges from elastomer treated beads. The principal crack is associated with many secondary cracks around coated particles showing crack deviation (Fig. 5b, c and d). So, the introduction of an elastomeric interlayer greatly changes the crack propagation in the composite material in comparison with untreated glass beads (Fig. 5a). With this treatment, the work of fracture increases, as revealed by intrinsic parameters. The value of  $K_{Ic}$  arises from a greater extent of energy dissipation through deformation in the vicinity of the tips. These deformation processes are probably the same as in rubber modified material: microvoiding in rubbery interphase and multiple

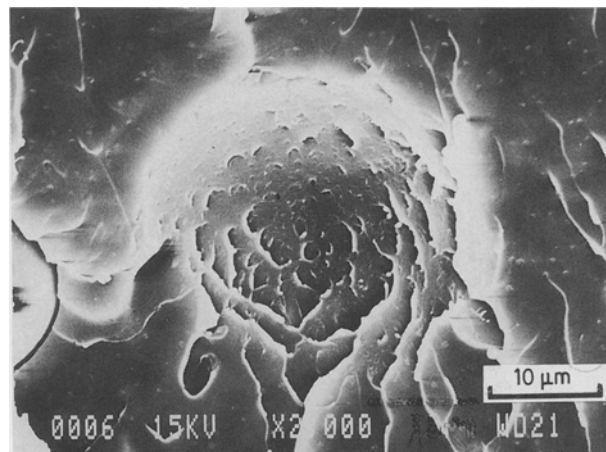


Figure 6 Micrograph of the fracture surface of an SEN specimen for the "optimum" thickness (2.8% for  $e/r$ ) of the elastomeric interlayer.

localized shear yielding. This last process is initiated by stress concentrations which could be explained by the stress distributions computed by Ricco. SEM observations also show a maximum in the number of secondary cracks in the matrix and around coated glass beads at the "optimum" thickness (2.8% maximum in fracture properties  $K_{Ic}$ ,  $G_{Ic}$ ) (Fig. 6). The improvement of  $K_{Ic}$  with the simultaneous decrease of the work-hardening rate  $K/M$  clearly correlates the toughening effect to the localized shear yielding mechanism.

#### 4. Conclusions

In agreement with previous work on glass beads composites, the critical stress intensity factors  $K_{Ic}$  of glass beads/(DGEBA-*DDA*) matrix composites increases with volume fraction of filler via crack front pinning mechanism. An influence of particle size on elastic, pre-yielding and fracture properties is also displayed.

With a CTBN based adduct, a crosslinked coating around glass beads is realized with various thicknesses up to  $(e/r) = 6.5\%$ . With such a surface treatment at 20% volume fraction of filler, a strong toughening effect is seen (the value of  $K_{Ic}$  reaches  $2.3 \text{ MPa m}^{1/2}$  compared to 1.88 for an uncoated glass bead based composite).

In agreement with theoretical models, an optimum thickness of elastomeric interlayer is experimentally determined (between 2 and 2.8% for  $(e/r)$ ). This maximum is correlated with a sharp decrease of  $K/M$  (work-hardening rate/compression modulus) determined in the pre-yielding stage. The toughening induced by this rubbery interlayer is achieved by promoting shear yielding in a localized zone in the vicinity of the crack tip. These conclusions are in a good agreement with fracture surface observations by SEM. The importance of elastomer localization is shown by designing a hybrid particulate composite: with 20% volume fraction of glass beads, the same amount of rubber is dissolved in the matrix as the quantity previously deposited around beads (at the maximum of improvement). A composite without rubber separations in the epoxy matrix is obtained. Similar values of  $T_g$  ( $143^\circ \text{C}$ ) and Young's modulus (4.56 GPa) as for composites based on coated glass beads are displayed



but  $K_{Ic}$  is only about  $1.85 \text{ MPa m}^{1/2}$ . For the same elastomer content, it demonstrates that the localization of rubber around glass beads greatly improved the fracture properties. Work is now in progress to study these composites in impact tests with high strain rates.

### Acknowledgements

The authors would like to thank Professor J. P. Pascault for his very helpful suggestions and Dr X. Caux for his help in work-hardening rate measurements.

### References

1. J. SPANOUDAKIS and R. J. YOUNG, *J. Mater. Sci.* **19** (1984) 473.
2. *Idem, ibid.* **19** (1984) 487.
3. S. SAHU and L. J. BROUTMAN, *Polym. Engng Sci.* **12** (2) (1972) 91.
4. L. J. BROUTMAN and S. SAHU, *Mater. Sci. Engng* **8** (1971) 98.
5. A. C. MOLONEY, H. H. KAUSCH, T. KAISER and H. R. BEER, *J. Mater. Sci.* **22** (1987) 381.
6. A. C. ROULIN-MOLONEY, W. J. CANTWELL and H. H. KAUSCH, *Polym. Comp.* **8** (5) (1987) 314.
7. G. LANDON, G. LEWIS and G. F. BODEN, *J. Mater. Sci.* **12** (1977) 1605.
8. H. ISHIDA and G. KUMAR, in "Molecular Characterization of Composites Interfaces" (Plenum Press, New York, 1983).
9. S. H. MORRELL, *Rubber Proc. Appl.* **1** (1981) 179.
10. R. J. YOUNG, in "Structural Adhesives" (edited by A. J. Kinloch (Elsevier, New York, 1986) p. 163.
11. J. N. SULTAN and F. J. MCGARRY, *Polym. Engng Sci.* **13** (1973) 29.
12. A. J. KINLOCH, D. L. MAXWELL and R. J. YOUNG, *J. Mater. Sci.* **20** (1985) 4169.
13. R. J. YOUNG, D. L. MAXWELL and A. J. KINLOCH, *ibid.* **21** (1986) 380.
14. D. L. MAXWELL, R. J. YOUNG and A. J. KINLOCH, *J. Mater. Sci. Lett.* **3** (1984) 9.
15. V. A. MATONIS and N. C. SMALL, *Polym. Engng Sci.* **9** (2) (1969) 90.
16. L. J. BROUTMAN and B. D. AGARWAL, *ibid.* **14** (1974) 581.
17. T. RICCO, A. PAVAN, F. DANUSSO, *ibid.* **18** (10) (1978) 774.
18. M. E. T. DEKKERS, J. P. M. DORTMANS and D. HEIKENS, *Polym. Commun.* **26** (1985) 145.
19. G. F. ABATE and D. HEIKENS, *ibid.* **24** (1983) 137.
20. G. C. EASTMOND and G. MUCCIARELLO, *Polymer* **23** (1982) 164.
21. A. T. DIBENEDETTO and L. NICOLAIS, in "Interfaces in Composites" (Advances in Composite Materials), edited by G. Piatti (Applied Science Publishers Ltd, London, 1978) p. 153.
22. R. S. RAGHAVA, *J. Polym. Sci.* **B25** (1987) 1017.
23. D. G. PEIFFER and L. E. NIELSEN, *J. Appl. Polym. Sci.* **23** (1979) 2253.
24. B. SCHLUND and M. LAMBLA, *Polym. Composites* **6** (4) (1985) 272.
25. G. RIESS, M. BOURDEAUX, M. BRIE and G. JOUQUET, in Proceedings of the 2nd Carbon Fibres Conference (Plastics Institute, London, 1974).
26. Y. G. LIN, J. F. GERARD, J. Y. CAVAILLE, H. SAUTERAU and J. P. PASCAULT, *Polym. Bull.* **17** (1987) 97.
27. Y. G. LIN, J. P. PASCAULT and H. SAUTERAU, in "Polymer Composites" (W. De Gruyter, Berlin, 1986) p. 373.
28. J. F. GERARD, *Polym. Engng Sci.* **28** (9) (1988) 568.
29. N. AMDOUNI, H. SAUTERAU and J. F. GERARD (to be published).
30. Y. G. LIN, J. GALY, H. SAUTERAU and J. P. PASCAULT, in "Crosslinked Epoxies", edited by B. Sedlacek (W. de Gruyter, Berlin, 1987) p. 148.
31. A. J. KINLOCH and R. J. YOUNG, in "Fracture Behavior of Polymers" (Applied Science Publishers, London, 1983).
32. B. ESCAIG, in "Plastic Deformation of Amorphous and Semi-Crystalline Materials", edited by B. Escaig and C. G'Sell (Les Editions de Physique, Les Ullis, 1982) p. 187.
33. J. M. LEFEBVRE, C. BUTEL and B. ESCAIG, *J. Mater. Sci.* **19** (1984) 2415.
34. X. CAUX, G. COULON and B. ESCAIG, *Polymer* **27** (1986) 1749.
35. J. A. MANSON and L. H. SPERLING, in "Polymer Blends and Composites" (Plenum Press, New York, 1976).
36. O. ISHAI and L. J. COHEN, *J. Comp. Mater.* **2** (1968) 302.
37. A. C. MOLONEY, H. H. KAUSCH and H. R. STIEGER, *J. Mater. Sci.* **18** (1983) 208.
38. F. F. LANGE and K. C. RADFORD, *J. Mater. Sci.* **6** (1971) 1197.
39. A. C. MOLONEY, H. H. KAUSCH and H. R. STIEGER, *J. Mater. Sci.* **19** (1984) 1125.
40. A. J. KINLOCH and J. G. WILLIAMS, *J. Mater. Sci.* **15** (1980) 987.
41. A. C. ROULIN-MOLONEY, N. CUDRE-MAUROUX and H. H. KAUSCH, *Polym. Composites* **8** (5) (1987) 324.
42. A. J. KINLOCH, S. J. SHAW, D. A. TOD and D. L. HUNSTON, *Polymer* **24** (1983) 1341.

Received 20 October 1988  
and accepted 10 April 1989